Boosting CNS axon regeneration by harnessing antagonistic effects of GSK3 activity

Marco Leibinger[a], Anastasia Andreadaki[a], Renate Golla[a], Evgeny Levin[a], Alexander M. Hilla[a], Heike Diekmann[a], and Dietmar Fischer[a,1]

[a]Division of Experimental Neurology, Department of Neurology, Heinrich Heine University of Düsseldorf, 40225 Duesseldorf, Germany

Edited by Mark H. Tuszynski, University of California, San Diego, La Jolla, CA, and accepted by Editorial Board Member Fred H. Gage May 11, 2017 (received for review December 30, 2016)

Implications of GSK3 activity for axon regeneration are often inconsistent, if not controversial. Sustained GSK3 activity in GSK3$^{S/A}$ knock-in mice reportedly accelerates peripheral nerve regeneration via increased MAP1B phosphorylation and concomitantly reduces microtubule detyrosination. In contrast, the current study shows that lens injury-stimulated optic nerve regeneration was significantly compromised in these knock-in mice. Phosphorylation of MAP1B and CRMP2 was expectedly increased in retinal ganglion cell (RGC) axons upon enhanced GSK3 activity, but, surprisingly, no GSK3-mediated CRMP2 inhibition was detected in sciatic nerves, thus revealing a fundamental difference between central and peripheral axons. Conversely, genetic or shRNA-mediated conditional KO/knockdown of GSK3β reduced inhibitory phosphorylation of CRMP2 in RGCs and improved optic nerve regeneration. Accordingly, GSK3β KO-mediated neurite growth promotion and myelin disinhibition were abrogated by CRMP2 inhibition and largely mimicked in WT neurons upon expression of constitutively active CRMP2 (CRMP2$^{T/A}$). These results underscore the prevalent requirement of active CRMP2 for optic nerve regeneration. Strikingly, expression of CRMP2$^{T/A}$ in GSK3$^{S/A}$ RGCs further boosted optic nerve regeneration, with axons reaching the optic chiasm within 3 wk. Thus, active GSK3 can also markedly promote axonal growth in central nerves if CRMP2 concurrently remains active. Similar to peripheral nerves, GSK3-mediated MAP1B phosphorylation/activation and the reduction of microtubule detyrosination contributed to this effect. Overall, these findings reconcile conflicting data on GSK3-mediated axon regeneration. In addition, the concept of complementary modulation of normally antagonistically targeted GSK3 substrates offers a therapeutically applicable approach to potentiate the regenerative outcome in the injured CNS.

CNS | axon regeneration | GSK3 | CRMP2 | MAP1B

Mature neurons of the CNS such as retinal ganglion cells (RGCs) are normally unable to regenerate injured axons because of the inhibitory environment for axonal growth cones (e.g., myelin) as well as their insufficient intrinsic capability to enter a regenerative axonal growth program (1–3). Thus, CNS injuries normally lead to an irreversible functional loss, such as paralysis after spinal cord injury or blindness after optic nerve damage, respectively. During the past two decades, various treatments have been identified to transfer adult RGCs into an active regenerative state. For example, induction of an inflammatory stimulation (IS) via lens injury is neuroprotective and enables moderate axon growth beyond the injury site of the optic nerve (4–9). These effects are mostly mediated by increased retinal expression of cytokines, such as CNTF, LIF, and IL-6 (4, 5, 8). These cytokines then activate or modulate signaling pathways in injured RGCs relevant for regeneration, such as JAK/STAT3 and mTOR (10–13). Despite this activation of the intrinsic state, RGCs are still sensitive toward inhibitory myelin (10, 14). Thus, combinatorial approaches that overcome inhibitory myelin signaling further improve IS-mediated axon regeneration into the optic nerve (10, 14–16).

It is now undisputed that glycogen synthase kinase 3 (GSK3) is crucially involved in regenerative processes upon axonal injury. However, data from several laboratories are conflicting, and the exact role of GSK3 in CNS axon regeneration remains controversial. Whereas some studies reported that inhibition of GSK3 would promote axonal growth or myelin disinhibition, others claimed exactly the opposite (17–22). It is conceivable that the role of GSK3 might differ depending on cell type, neuronal age, or axonal environment, which impedes comparisons of results from different studies (23). In addition, GSK3 is known to influence the activity of multiple downstream targets and could hence adopt not just one, but several, potentially diverse functions in the context of nerve regeneration. For instance, many microtubule-binding proteins, such as collapsin response mediator protein 2 (CRMP2) and microtubule-associated protein 1B (MAP1B), are validated GSK3 substrates and may affect microtubule assembly and dynamics differently. CRMP2, which is inhibited by GSK3-mediated phosphorylation, reportedly promotes microtubule polymerization and myelin disinhibition (20, 24, 25). As for most GSK3 substrates, CRMP2 inactivation via GSK3 requires prior priming by distinct kinases, such as cyclin-dependent kinase 5 (CDK5) (26). In contrast, MAP1B is directly activated by GSK3-mediated phosphorylation without prior priming and has been suggested to promote axon growth (22, 27, 28). Moreover, investigations into the role of GSK3 in axon regeneration are full of potential pitfalls. Pharmacological GSK3 inhibitors with different mechanisms of action might yield inconsistent results, and even the extent of GSK3 inhibition seems to influence experimental outcomes, not to mention off-target effects (29, 30). Finally, ectopic expression might

Significance

The role of GSK3 in axon regeneration is controversial. Whereas increased GSK3 activity accelerates peripheral nerve regeneration, it shows the opposite effect in the CNS. Moreover, KO/knockdown of GSK3β in growth-stimulated retinal ganglion cells (RGCs) was disinhibitory and potentiated optic nerve regeneration. This dichotomy was the result of a GSK3-dependent and CNS-specific inhibition of axonal CRMP2, which compromised RGCs' ability for axon growth. As GSK3 inhibition, neuronal expression of constitutively active CRMP2 (CRMP2$^{T/A}$) potentiated optic nerve regeneration and, strikingly, unmasked an axon growth-promoting effect of active GSK3 as in peripheral nerves. CRMP2$^{T/A}$ expression and GSK3 activation additively enabled extensive optic nerve regeneration, thereby reconciling conflicting data in GSK3-mediated axon regeneration and opening novel treatment possibilities for CNS repair.

Author contributions: M.L. and D.F. designed research; M.L., A.A., R.G., E.L., A.M.H., and D.F. performed research; M.L., A.A., A.M.H., R.G., and D.F. analyzed data; and M.L., H.D., and D.F. wrote the paper.

The authors declare no conflict of interest.

This article is a PNAS Direct Submission. M.H.T. is a guest editor invited by the Editorial Board.

[1]To whom correspondence should be addressed. Email: dietmar.fischer@uni-duesseldorf.de.

This article contains supporting information online at www.pnas.org/lookup/suppl/doi:10.1073/pnas.1621225114/-/DCSupplemental.

www.pnas.org/cgi/doi/10.1073/pnas.1621225114

result in nonphysiological GSK3 activity levels with potentially adverse effects, and the focus upon one of the two GSK3 isoforms, most notably GSK3β, could elicit compensatory responses of GSK3α and vice-versa.

We previously used well-defined mice with phosphorylation-resistant GSK3α^{S21A}/β^{S9A} [GSK3(α/β)$^{S/A}$] double knock-in as well as respective single knock-ins (31) to unambiguously investigate the effect of GSK3 on peripheral nerve regeneration (32). Elevated GSK3 activity in these mice led to markedly accelerated axon regeneration after sciatic nerve injury (22, 32). This effect was based on a phospho-MAP1B (pMAP1B)-associated inhibition of microtubule detyrosination and subsequent increase of microtubule dynamics in axonal growth cones (22, 32). Thus, elevated GSK3 activity promotes axon regeneration in the adult peripheral nervous system (PNS).

Here, we used the same transgenic animals as well as conditional RGC-specific GSK3α and GSK3β KOs to study the role of both GSK3 isoforms on adult optic nerve regeneration. Surprisingly, elevation of GSK3 activity in GSK3$^{S/A}$ mice compromised, and GSK3β KO (GSK3β$^{-/-}$) potentiated, IS-stimulated regeneration. These effects were associated with varying levels of inactive CRMP2 in optic nerve axons, whereas CRMP2 phosphorylation was barely detectable in PNS axons. The essential role of CRMP2 in GSK3-mediated RGC axon regeneration was confirmed by using various in vivo and in vitro assays. However, as in the PNS, elevated GSK3 activity enhanced neurite growth of RGCs in experimental settings with constant CRMP2 activity, indicating that CRMP2 inhibition masks the positive effect of MAP1B activity in CNS neurons. Consequently, RGC-specific expression of constitutively active CRMP2, combined with enhanced GSK3 activity, boosted IS stimulated optic nerve regeneration considerably more than GSK3β$^{-/-}$, with some axons reaching the optic chiasm as soon as 3 wk after injury. Thus, differential regulation of selected GSK3 targets can markedly improve the regenerative outcome and could therefore provide treatment strategies for the injured CNS.

Results

Inhibition of GSK3 in Injured RGCs. Sciatic nerve crush reportedly induces inhibitory GSK3 phosphorylation in adult dorsal root ganglion (DRG) sensory neurons (22). To test whether GSK3 is similarly inhibited in injured CNS neurons, we first examined the levels of phosphorylated GSK3 in RGCs before and after optic nerve crush (ONC). Although retinal flat-mounts of untreated WT mice showed only few phospho-serine-21-GSK3α (pGSK3α)- and phospho-serine-9-GSK3β (pGSK3β)-positive RGCs, numbers and intensities of pGSK3-stained neurons were obviously increased 5 d after ONC, whereas levels of total GSK3 remained unaffected (Fig. 1*A*). Costaining with a βIII-tubulin antibody localized pGSK3α and pGSK3β in RGCs and their axons in the ganglion cell layer, whereas other retinal layers revealed only weak staining unaltered by ONC. Absence of pGSK3 signals in retinal flat-mounts of nonphosphorylatable GSK3(α/β)$^{S/A}$ knock-in mice (31) verified the staining specificity of these pGSK3 antibodies (Fig. 1*A*). Western blot analyses confirmed induction

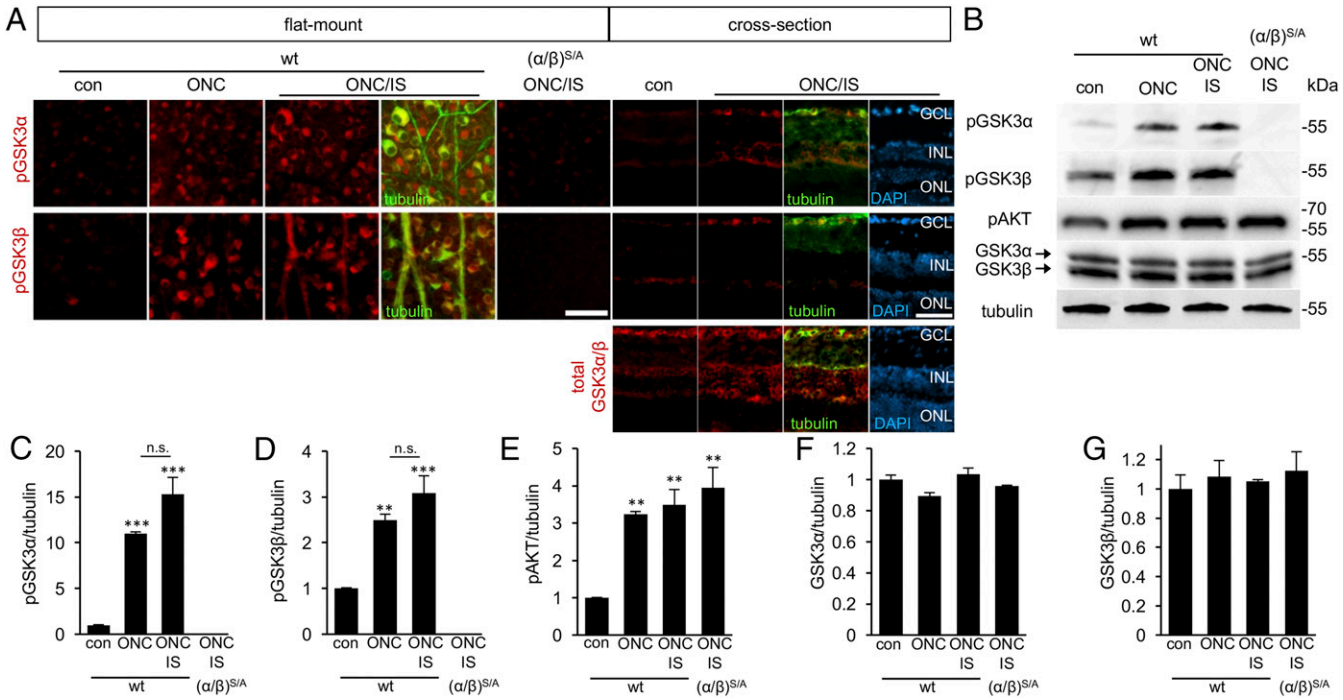

Fig. 1. ONC elicits inhibitory GSK3α and GSK3β phosphorylation in RGCs. (*A*) Retinal flat-mounts and cross-sections of WT mice isolated 5 d after ONC and ONC+IS, respectively. Compared with untreated mice (con), S21-phosphorylation of GSK3α (pGSK3α; red) and S9-phosphorylation of GSK3β (pGSK3β; red) were similarly increased in βIII-tubulin–positive RGCs (green) after ONC and ONC+IS. Retinal cross-sections reveal that GSK3α/β phosphorylation occurred in RGCs in the ganglion cell layer (GCL). Total GSK3α/β (red) remained unchanged. Phospho-GSK3 staining was absent in retinae of GSK3(α/β)$^{S/A}$ knock-in [(α/β)$^{S/A}$] mice, indicating antibody specificity. Nuclei were labeled by DAPI (blue). INL, inner nuclear layer; ONL, outer nuclear layer. (Scale bars: 50 μm.) (*B*) Western blots of retinal lysates from WT mice untreated (con), 5 d after ONC or ONC+IS. pGSK3α and pGSK3β signals increased after ONC compared with untreated controls, but additional IS did not further enhance GSK3 phosphorylation. No pGSK3 signals were detected in retinal lysates from (α/β)$^{S/A}$ mice, verifying antibody specificities. Levels of T308-phosphorylated AKT (pAKT) were elevated after injury in WT and (α/β)$^{S/A}$ mice. Total GSK3α and GSK3β levels were comparable in all experimental groups. βIII-tubulin served as a loading control. (*C*–*G*) Densitometric quantification of pGSK3α (*C*), pGSK3β (*D*), pAKT (*E*), total GSK3α (*F*), and total GSK3β (*G*) relative to βIII-tubulin and normalized to WT control on different Western blots as depicted in *B*. Significances of intergroup differences were evaluated by one-way ANOVA with Tukey post hoc test. Treatment effects compared with WT control: $^{**}P < 0.01$ and $^{***}P < 0.001$. n.s., nonsignificant. Values represent means ± SEM of $n = 3$–4 retinae per group.

of GSK3α and GSK3β phosphorylation upon nerve injury, whereas total expression of both isoforms remained unchanged (Fig. 1 *B–D*, *F*, and *G*). Phosphorylation of AKT, an upstream mediator of this inhibitory GSK3 phosphorylation, was similarly increased upon ONC (Fig. 1 *B* and *E*). However, neither AKT nor GSK3 phosphorylation were further increased in the proregenerative condition of IS compared with ONC alone (Fig. 1 *A–G*). Furthermore, ONC- and particularly IS-mediated induction of the regeneration-associated genes growth-associated protein 43 (gap43), galanin, and small proline-rich protein 1 a (sprr1a) were unaffected by GSK3$(\alpha/\beta)^{S/A}$ knock-in or GSK3$\beta^{-/-}$ (Fig. S1). Thus, the IS-mediated increase of the regenerative capacity of RGCs is seemingly independent of GSK3 activity.

Compromised RGC Axon Regeneration upon Sustained GSK3 Activity. By using GSK3$(\alpha/\beta)^{S/A}$ knock-in mice, we recently showed that sustained GSK3 activity reduced microtubule detyrosination, thereby markedly accelerating axon regeneration and functional recovery of the regeneration-competent sciatic nerve (22, 32). The findings that regeneration-stimulatory IS did not affect the levels of GSK3 phosphorylation in RGCs (Fig. 1) and, on the contrary, GSK3$^{S/A}$ or GSK3$\beta^{-/-}$ did not influence IS-induced expression of regeneration-associated genes provided us the unique opportunity to use this approach to investigate the contribution of GSK3 in CNS regeneration. To this end, we subjected WT, GSK3$\alpha^{S/A}$, GSK3$\beta^{S/A}$, and GSK3$(\alpha/\beta)^{S/A}$ mice to ONC or ONC+IS. We then (*i*) cultured dissociated retinal cells 5 d after surgery for 24 h to investigate spontaneous neurite growth (reflecting the regenerative state) or (*ii*) quantified regenerating axons in the distal optic nerve at 3 wk after surgery to test the effect on axon regeneration in vivo (Fig. 2). Unexpectedly, spontaneous neurite growth of in vivo-stimulated RGCs was markedly reduced in cultures of all three GSK3 knock-in genotypes compared with WT controls (Fig. 2 *A* and *B*), even though levels of phospho-MAP1B were enhanced in neurite growth cones of GSK3$\alpha^{S/A}$ and GSK3$\beta^{S/A}$ RGCs and even stronger in neurons with GSK3$(\alpha/\beta)^{S/A}$ compared with WT controls (Fig. 2*C*). Similarly, optic nerve regeneration, particularly at long distances, was significantly reduced in these transgenic mice compared with respective IS-treated WT controls (Fig. 2 *D–I* and Fig. S2). Quantification of surviving RGCs 3 wk after ONC+IS in retinal flat-mounts revealed similar numbers for all genotypes (Fig. S3 *A* and *B*), indicating that differences in optic nerve regeneration were not attributable to distinct effects on neuroprotection. After ONC alone, neurite growth of cultured RGCs as well as optic nerve regeneration in vivo was generally strongly limited. Therefore, we were not able to detect significant differences in GSK3$\alpha^{S/A}$, GSK3$\beta^{S/A}$, and GSK3$(\alpha/\beta)^{S/A}$ genotypes compared with respectively treated WT controls.

Potentiation of IS-Induced Optic Nerve Regeneration upon GSK3β KO. As sustained GSK3 activity compromised optic nerve regeneration, we investigated next whether inhibition of GSK3 by conditional KO might have the opposite effect. To this end, AAV-Cre was injected into eyes of adult GSK3α- or GSK3β-floxed mice to specifically delete GSK3α (GSK3$\alpha^{-/-}$) or GSK3β (GSK3$\beta^{-/-}$) in RGCs, whereas WT controls received AAV-GFP. Generally, more than 90% of RGCs were successfully transduced, and specific KO of GSK3α or GSK3β was verified by immunohistochemical staining (Fig. S4 *A* and *B*). Axon regeneration 3 wk after ONC alone was only moderately increased upon GSK3$\beta^{-/-}$ compared with the WT (Fig. 3 *A* and *E* and Fig. S5 *A* and *B*), whereas GSK3$\alpha^{-/-}$ had no effect. In parallel, we also analyzed the effect of this genetic manipulation in mice with IS-mediated increased RGC growth capacity. In comparison with sole ONC, additional IS treatment expectedly elicited moderate nerve regeneration, which was strikingly potentiated upon GSK3$\beta^{-/-}$ but not GSK3$\alpha^{-/-}$ (Fig. 3 *A–C* and *E* and Fig. S5 *C–E*). To confirm this effect of reduced GSK3β activity in WT animals, we also generated a GSK3β-shRNA–encoding AAV. This AAV showed a somewhat generally lower transduction rate (~70%) compared with AAV-Cre, but efficiently and specifically suppressed endogenous GSK3β in transduced RGCs (Fig. S4*C*). Significantly, shRNA-mediated GSK3β knockdown also markedly increased IS-induced optic nerve regeneration (Fig. 3 *A*, *D*, and *E* and Fig. S5*F*). This proregenerative effect of reduced GSK3β activity was again

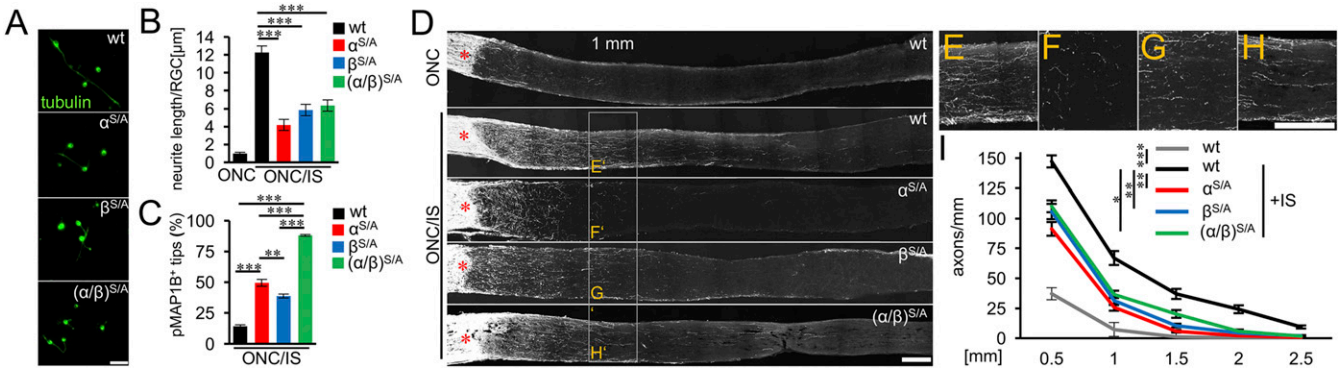

Fig. 2. GSK3$^{S/A}$ reduces IS-induced optic nerve regeneration. (*A*) Representative images of βIII-tubulin–positive RGCs from WT, GSK3$\alpha^{S/A}$ ($\alpha^{S/A}$), GSK3$\beta^{S/A}$ ($\beta^{S/A}$), and GSK3$(\alpha/\beta)^{S/A}$ [$(\alpha/\beta)^{S/A}$] knock-in mice, respectively, after 24 h in culture. Animals received ONC and IS 5 d before culture preparation to transform neurons into an axon growth mode. (Scale bar: 50 µm.) (*B*) Quantification of spontaneous neurite growth in cultures as described in *A*. RGC neurite length of WT mice that received ONC but no IS was included to visualize the growth-promoting effect of IS. In comparison with WT RGCs, neurite growth of $\alpha^{S/A}$, $\beta^{S/A}$, and $(\alpha/\beta)^{S/A}$ RGCs was markedly compromised. Values represent means ± SEM from $n = 3$ independent experiments. (*C*) Quantification of the percentage of phospho-MAP1B (pMAP1B)-positive axon tips in RGC cultures as depicted in *A*. $\alpha^{S/A}$ and $\beta^{S/A}$ significantly increased the percentage of positive tips, with the strongest effects in $(\alpha/\beta)^{S/A}$ RGCs compared with WT controls. Data represent means ± SEM of $n = 3$ independent experiments. (*D*) Representative longitudinal optic nerve sections (collages of single photos) from WT, $\alpha^{S/A}$, $\beta^{S/A}$, and $(\alpha/\beta)^{S/A}$ knock-in mice with regenerating, cholera toxin β-subunit (CTB)-labeled axons 21 d after ONC+IS. A nerve from a WT mouse 21 d after sole ONC was included as reference for IS-mediated regeneration. Lesion sites are indicated by asterisks. (Scale bar: 200 µm.) (*E–H*) Higher magnifications of respective optic nerve sections 1 mm distal to the injury site as indicated in *D*. (Scale bar: 200 µm.) (*I*) Quantification of regenerating axons per millimeter of optic nerve width at 0.5, 1, 1.5, 2, and 2.5 mm beyond the lesion site in treatment groups as in *D*. Compared with WT animals, IS-triggered optic nerve regeneration was distinctly compromised in $\alpha^{S/A}$, $\beta^{S/A}$ knock-in mice and more slightly upon α+β knock-in $(\alpha/\beta)^{S/A}$. Values represent means ± SEM of $n = 6–8$ animals per experimental group. Significances of intergroup differences in *B*, *C*, and *I* were evaluated by one-way ANOVA with Tukey or Holm–Šídák post hoc test. Treatment effects: $^*P < 0.05$, $^{**}P < 0.01$, and $^{***}P < 0.001$.

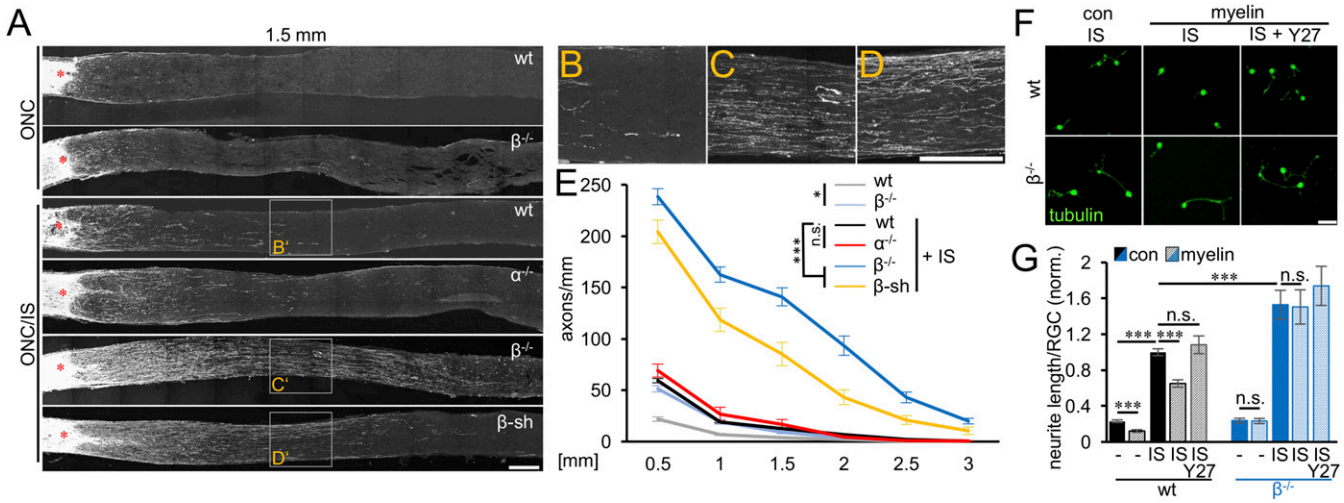

Fig. 3. Conditional RGC-specific GSK3β KO potentiates IS-induced optic nerve regeneration and confers disinhibition. (*A*) Longitudinal optic nerve sections (collages of single photos) with regenerating, CTB-labeled axons prepared from WT mice, upon conditional, RGC-specific GSK3α ($\alpha^{-/-}$) or GSK3β ($\beta^{-/-}$) KO, or upon shRNA-mediated GSK3β knockdown (β-sh) 21 d after ONC or ONC+IS. Lesion sites are indicated by asterisks. (Scale bar: 200 μm.) (*B–D*) Higher magnifications of respective optic nerve sections 1.5 mm beyond the lesion site as indicated in *A*. (Scale bar: 200 μm.) (*E*) Quantification of regenerating axons per millimeter of optic nerve width at 0.5, 1, 1.5, 2, 2.5, and 3 mm beyond the lesion site from treatment groups as in *A*. RGC-specific $\beta^{-/-}$ only moderately increased axonal regeneration, but strongly potentiated IS-induced optic nerve regeneration, whereas $\alpha^{-/-}$ had no effect. β-sh reproduced the effect of $\beta^{-/-}$. Values represent means ± SEM of n = 6–8 animals per group. (*F*) Representative images of in vivo pretreated (ONC+IS 5 d before tissue preparation), βIII-tubulin–positive RGCs from WT mice or animals with $\beta^{-/-}$ after 1 d in culture on a growth-permissive (con) or inhibitory (myelin) substrate. Some of the cultures were additionally treated with Y27632 (Y27; 10 μM), which served as a positive control for disinhibition. (Scale bar: 50 μm.) (*G*) Quantification of neurite length per RGC as described in *F* in comparison with ONC-treated RGCs (–). $\beta^{-/-}$ significantly enhanced neurite growth on permissive substrate (con) only after ONC+IS treatment and not after ONC, but overcame myelin-mediated growth inhibition in both conditions, similar to Y27. Values were normalized against the WT IS control group with an average neurite length of 6.94 μm per RGC and represent means ± SEM of at least three independent experiments per experimental group. Significances of intergroup differences in *E* and *G* were evaluated using two-way (*E*) or three-way (*G*) ANOVA with Tukey post hoc test. Treatment effects: $*P < 0.05$ and $***P < 0.001$. n.s., nonsignificant.

independent of RGC survival, as their numbers were comparable between respective experimental groups (Fig. S6 *A* and *B*).

To elucidate conceptual mechanism(s) that might underlie the markedly increased regeneration mediated by GSK3β inactivation, axon growth of in vivo-stimulated RGCs was analyzed in more detail in cell culture. Plating RGCs on different substrates allowed us to distinguish between effects on neurite growth per se and disinhibition toward inhibitory molecules present in the optic nerve, such as CNS myelin (11, 15). When retinal cells were dissociated 5 d after sole ONC and cultured for 24 h, neurite growth was expectedly limited, and no significant difference in neurite length was determined between RGCs from WT and GSK3$\beta^{-/-}$ mice (Fig. 3*G*). However, growth inhibition mediated by CNS myelin extract was observed only for WT, but not GSK3$\beta^{-/-}$ RGCs, suggesting that GSK3$\beta^{-/-}$ mostly acts in a disinhibitory manner rather than increasing the regenerative capacity. As in vivo, growth in culture was significantly increased upon ONC+IS in both genotypes and ∼1.5 times higher for GSK3$\beta^{-/-}$ than in WT RGCs (Fig. 3 *F* and *G*). In addition, neurite extension was again significantly reduced in WT, but not GSK3$\beta^{-/-}$ RGCs on myelin. Similarly, treatment of cultures with the ROCK inhibitor Y27632, which reportedly overcomes myelin inhibition (15, 33, 34), rescued myelin-mediated growth reduction in WT, but did not further increase neurite growth of GSK3$\beta^{-/-}$ RGCs (Fig. 3*G*). Thus, GSK3$\beta^{-/-}$ moderately further promoted neurite elongation of IS-stimulated RGCs on a growth-permissive substrate and was disinhibitory toward CNS myelin, suggesting that these features underlie the potentiating effect on IS-stimulated optic nerve regeneration and explain the rather moderate effects after ONC alone (Fig. 3 *A* and *E*).

GSK3 Effects on Optic Nerve Regeneration Depend on CRMP2 Phosphorylation. As our results on optic nerve regeneration opposed our previous findings in the PNS (22, 32) and most GSK3 substrates require prior priming/phosphorylation by other kinases, we speculated that GSK3 substrates might be differentially regulated in the CNS and PNS. We previously noted that CRMP2 is hardly phosphorylated in sciatic nerves of WT and even GSK3 $(\alpha/\beta)^{S/A}$ mice with higher GSK3 kinase activity (32), and therefore tested whether CRMP2 phosphorylation may be differently regulated in axons of the optic nerve. Indeed, Western blot analysis revealed >10-fold higher phospho-CRMP2 (pCRMP2) levels in WT optic nerves than in sciatic nerves from the same animals or from GSK3$(\alpha/\beta)^{S/A}$ mice relative to βIII-tubulin, whereas levels of total CRMP2 protein were similar (Fig. 4 *A–C*). Immunohistochemical staining of optic nerve sections from WT and GSK3 $(\alpha/\beta)^{S/A}$ verified pCRMP2 expression in RGC axons (Fig. S7*C*), making CRMP2 a potential candidate to explain the opposite effects of GSK3 activity in the central and peripheral nervous system. We therefore analyzed CRMP2 phosphorylation in all GSK3 genotypes in more detail. Western blot analyses and immunohistochemistry verified similar levels of total CRMP2 in RGCs and their axons in WT and all $GSK3^{S/A}$ knock-in and GSK3 KO mice used in this study before and after ONC (Fig. 4 *D* and *F* and Figs. S7 *A* and *B* and S8 *D* and *E*). Expectedly, all constitutively active $GSK3^{S/A}$ genotypes showed increased axonal levels of pCRMP2 compared with WT mice (Fig. 4 *D* and *E* and Fig. S8*A*). As ONC reduced GSK3 activity (Fig. 1), pCRMP2 levels were expectedly decreased upon ONC and ONC+IS in WT mice. Although reductions were also observed in retinal axons and optic nerves of all three knock-in genotypes upon nerve injury, absolute pCRMP2 levels remained significantly higher compared with respective WT nerves (Fig. 4 *D* and *E* and Fig. S8*A*). Thus, modulation of GSK3 activities affected pCRMP2 levels in injured axons. Consistently, in KO mice, levels of pCRMP2 were reduced upon depletion of GSK3β and GSK3(α/β), but not GSK3α (Fig. 4 *F* and *G* and Fig. S8*B*). Axotomy expectedly reduced CRMP2 phosphorylation also in optic nerves of KO mice, whereas levels were

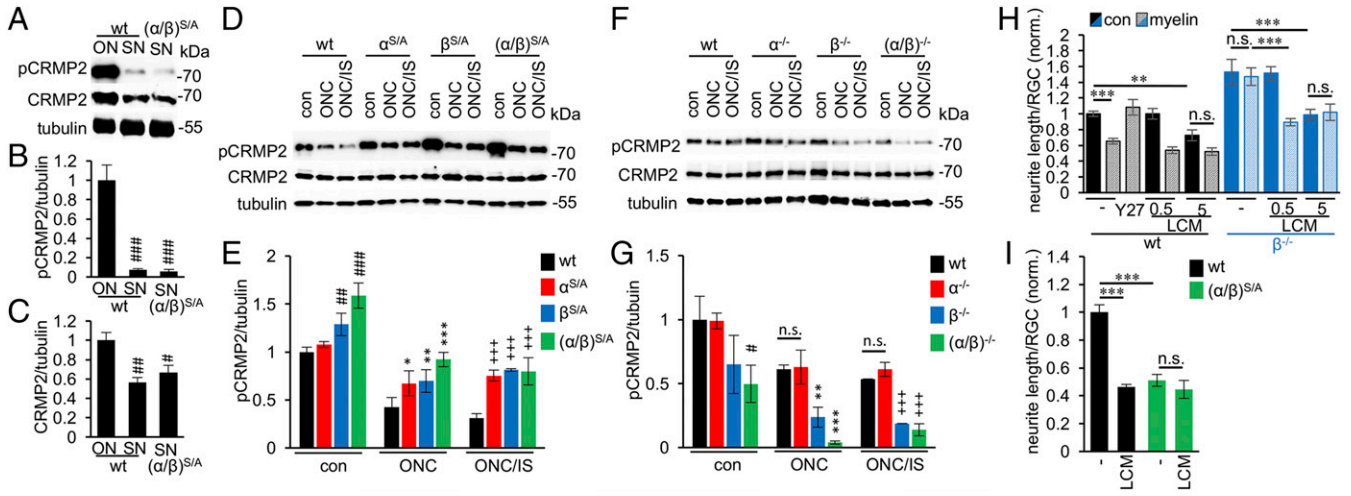

Fig. 4. CRMP2 phosphorylation in optic nerves of GSK3$^{S/A}$ or conditional GSK3 KOs correlates with axon regeneration. (*A*) Western blot analysis of T514-phosphorylated (pCRMP2) and total CRMP2 in sciatic nerves (SN) from untreated WT or GSK3$(\alpha/\beta)^{S/A}$ knock-in mice [$(\alpha/\beta)^{S/A}$] in comparison with untreated WT optic nerves (ON). βIII-tubulin (tubulin) was used as loading control. (*B* and *C*) Densitometric quantification of Western blots as in *A*. Relative to βIII-tubulin, approximately 10 times more pCRMP2 (*B*), but only approximately twice as much total CRMP2 (*C*), was detected in optic nerves compared with sciatic nerves. Values represent means ± SEM of $n = 3$ nerves per group. (*D*) Western blot analysis of pCRMP2 and total CRMP2 in optic nerve lysates from WT, GSK3$\alpha^{S/A}$ ($\alpha^{S/A}$), GSK3$\beta^{S/A}$ ($\beta^{S/A}$), and $(\alpha/\beta)^{S/A}$ knock-in mice that were left untreated (con) or subjected to ONC or ONC+IS, respectively, 5 d before tissue isolation. Only optic nerve segments proximal to the lesion site were used for the analysis. Levels of pCRMP2 were considerably decreased upon ONC and ONC+IS in WT animals but remained higher in $\alpha^{S/A}$, $\beta^{S/A}$, and $(\alpha/\beta)^{S/A}$ mice. Tubulin was used as loading control. (*F*) Western blot analysis of pCRMP2 and total CRMP2 in optic nerve lysates from GSK3α, GSK3β, or GSK3(α/β) floxed mice that were intravitreally injected with AAV-Cre [$\alpha^{-/-}$, $\beta^{-/-}$, $(\alpha/\beta)^{-/-}$] or AAV-GFP (WT). Three weeks thereafter, animals were subjected to treatments as described in *D*. RGC-specific $\beta^{-/-}$ or $(\alpha/\beta)^{-/-}$, but not $\alpha^{-/-}$ KO, reduced pCRMP2 levels compared with WT optic nerves in all three experimental conditions (control, ONC, and ONC+IS). Levels of total CRMP2 were unchanged among all treatment groups. Tubulin was used as loading control. (*E* and *G*) Densitometric quantification of pCRMP2 relative to tubulin on Western blots as depicted in *D* and *F*. To facilitate comparison between different genotypes, groups were arranged in a different order as in *D* and *E* (sorted by treatment, not by genotype). Values represent means ± SEM of $n = 3$–4 optic nerves per group. (*H*) Quantification of neurite growth of cultured RGCs from WT and $\beta^{-/-}$ mice treated with ONC+IS 5 d before culture preparation. Cultures were untreated (–) or incubated with Y27632 (Y27; 10 μM) or different concentrations of the CRMP2 inhibitor lacosamide (LCM, 0.5 or 5 μM) as indicated. Spontaneous neurite growth was evaluated in the absence (con) or presence of CNS myelin after 24 h in culture. Low concentrations of LCM (0.5 μM) did not affect RGC neurite growth on permissive substrate, but significantly compromised the disinhibitory effect of GSK3$\beta^{-/-}$. Higher LCM concentrations (5 μM) reduced neurite growth on permissive substrate in WT and GSK3$\beta^{-/-}$ RGCs, but showed no additional effect on myelin. Values represent means ± SEM of $n = 4$ independent experiments per group and were normalized to the WT control (–) with an average neurite length of 6.39 μm per RGC. (*I*) Quantification of neurite growth of RGCs from WT and $(\alpha/\beta)^{S/A}$ mice. Animals were subjected to ONC+IS 5 d before culture preparation. Cultures were untreated (–) or incubated with 5 μM LCM. LCM decreased neurite growth in WT but not $(\alpha/\beta)^{S/A}$ RGCs. Values represent means ± SEM of $n = 3$ independent experiments per group and were normalized to WT control (–) with an average neurite length of 12.27 μm per RGC. Significances of intergroup differences in *B*, *C*, *E*, *G*, *H*, and *I* were evaluated by one-way (*B* and *C*), two-way (*E*, *G*, and *I*), or three-way (*H*) ANOVA with Tukey post hoc test. Treatment effects were compared with WT control: $^{\#}P < 0.05$, $^{\#\#}P < 0.01$, $^{\#\#\#}P < 0.001$; WT ONC or as indicated: $^{*}P < 0.05$, $^{**}P < 0.01$, $^{***}P < 0.001$; and to WT ONC+IS: $^{+++}P < 0.001$. n.s., nonsignificant.

significantly lower in retinae and optic nerve lysates of GSK3$\beta^{-/-}$ and GSK3$(\alpha/\beta)^{-/-}$ mice, but not in GSK3$\alpha^{-/-}$ mice, compared with WT (Fig. 4 *F* and *G* and Fig. S8*B*). Immunohistochemical analysis of retinal flat-mounts upon GSK3(α/β) KO in AAV-Cre-transduced RGCs showed no detectable pCRMP2 signal in RGC somata and axons (Fig. S8 *B* and *C*), indicating that GSK3 activity is essential for CRMP2 phosphorylation. Thus, overall, this analysis of diverse GSK3 genotypes reveals a strong inverse correlation of pCRMP2 levels and the measured optic nerve regeneration in vivo.

To confirm a direct contribution of active CRMP2 to GSK3-mediated nerve regeneration, in vivo ONC+IS-stimulated retinal cells from WT, GSK3$\beta^{-/-}$, and GSK3$(\alpha/\beta)^{S/A}$ mice were cultured on growth-permissive substrate or inhibitory CNS myelin in the presence of the well-characterized CRMP2 inhibitor lacosamide (LCM) (35, 36). The disinhibitory effect of GSK3$\beta^{-/-}$ on neurite growth on myelin was already significantly reduced by 0.5 μM LCM, whereas 5 μM decreased the length of WT and GSK3$\beta^{-/-}$ neurites on growth-permissive substrate (Fig. 4*H*). On the contrary, LCM (5 μM) did not further compromise neurite elongation of GSK3$(\alpha/\beta)^{S/A}$ RGCs in similar cultures (Fig. 4*I*), as CRMP2 was already strongly phosphorylated and thereby inhibited after $(\alpha/\beta)^{S/A}$ knock-in. These data indicate that improved neurite extension and myelin disinhibition in GSK3$\beta^{-/-}$ RGCs depend on elevated CRMP2 activity (i.e., less phosphorylation), while enhanced CRMP2 inhibition by GSK3$(\alpha/\beta)^{S/A}$ compromises neurite growth of RGCs.

Potentiated Optic Nerve Regeneration upon Combinatorial Modulation of GSK3 Substrates. As the beneficial effects of GSK3$\beta^{-/-}$ depended on CRMP2 activity, we next tested whether exogenous expression of active CRMP2 may mimic the growth-potentiating effect of GSK3$\beta^{-/-}$ and reverse the negative effect of GSK3$(\alpha/\beta)^{S/A}$ on neurite growth in culture as well as axon regeneration in vivo. To this end, we expressed constitutively active CRMP2$^{Thr514/Ala}$ (CRMP2$^{T/A}$), which cannot be phosphorylated by GSK3, in WT and transgenic GSK3$(\alpha/\beta)^{S/A}$ mice. Intravitreal injection of this AAV transduced >70% of RGCs after 3 wk (Fig. S4*D*). Animals were then subjected to ONC+IS. First, we analyzed neurite growth of RGCs that had been isolated 5 d after surgery and cultured for 24 h on permissive substrate vs. inhibitory CNS myelin extract. As GSK3$\beta^{-/-}$ (Fig. 3*G*), expression of CRMP2$^{T/A}$ in WT RGCs slightly increased neurite growth per se and induced disinhibition toward myelin (Fig. 5*A*), providing further evidence that the effects of GSK3$\beta^{-/-}$ were predominantly mediated via increased CRMP2 activity. On the contrary, GSK3$(\alpha/\beta)^{S/A}$ expectedly reduced neurite growth, whereas myelin showed no additional inhibitory effect (Fig. 5*A*; similar as in WT RGCs treated with high

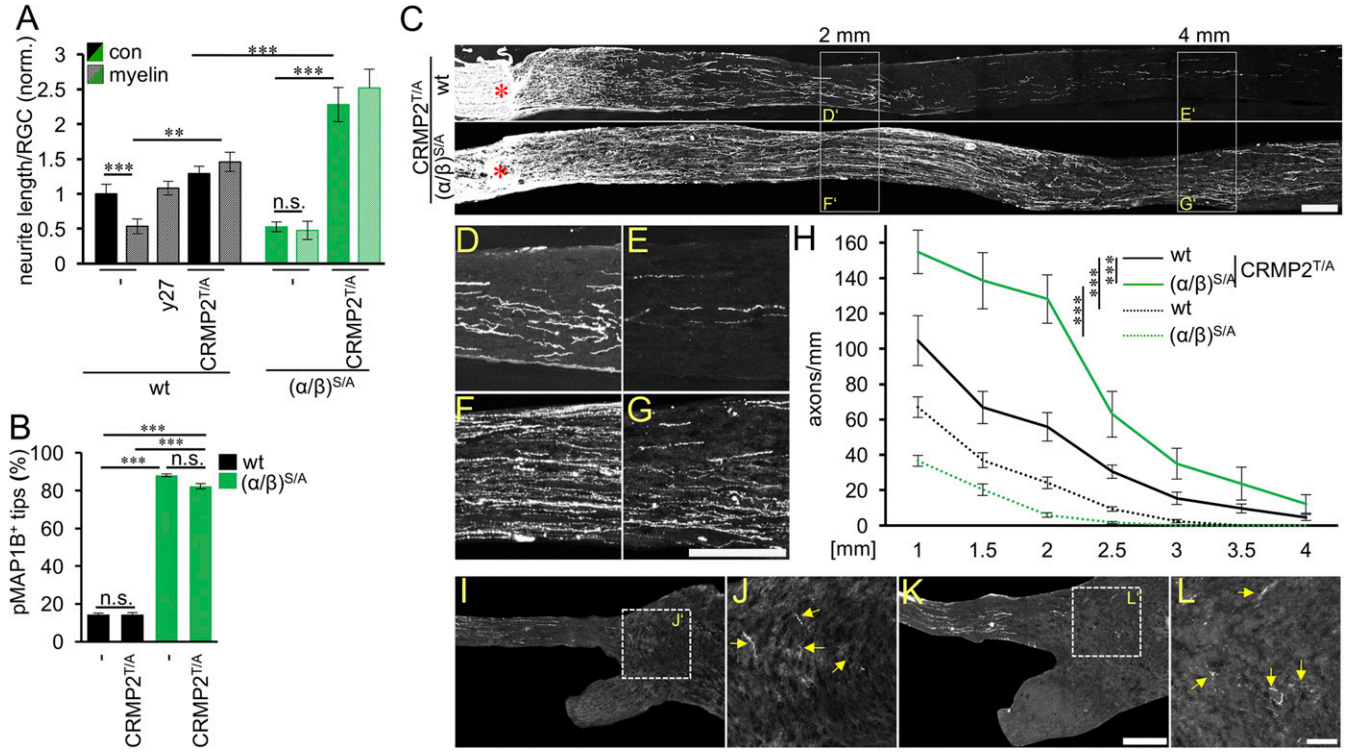

Fig. 5. Constitutively active CRMP2 promotes optic nerve regeneration. (*A*) Quantification of neurite growth of RGCs in retinal cultures of WT and GSK3$(\alpha/\beta)^{S/A}$ [$(\alpha/\beta)^{S/A}$] mice that were intravitreally injected with AAV-GFP (–) or AAV-CRMP2$^{T/A}$. Three weeks after AAV injection, animals were subjected to ONC+IS, and cultures prepared 5 d thereafter. Some of the cultures were incubated with 10 μM Y27632 (Y27). Spontaneous neurite growth was evaluated in the absence (con) or presence of CNS myelin after 24 h in culture. In WT RGCs, CRMP2$^{T/A}$ promoted myelin disinhibition and slight neurite growth. In $(\alpha/\beta)^{S/A}$ RGCs, CRMP2$^{T/A}$ reversed the neurite growth reducing effect of $(\alpha/\beta)^{S/A}$ and strongly potentiated neurite growth compared with respective WT cultures. Values represent means ± SEM of $n = 3$ independent experiments and were normalized to the WT control group (–) with an average neurite length of 4.52 μm per RGC. (*B*) Quantification of pMAP1B-positive neurite tips of RGCs as depicted in *A*. $(\alpha/\beta)^{S/A}$ significantly increased the percentage of pMAP1B-positive neurite tips compared with the WT. Expression of CRMP2$^{T/A}$ did not affected pMAP1B levels in WT or in $(\alpha/\beta)^{S/A}$ RGCs. Data represent means ± SEM of $n = 3$ independent experiments. (*C*) Representative longitudinal optic nerve sections (collages of single photographs) with regenerating, CTB-labeled axons prepared from WT or $(\alpha/\beta)^{S/A}$ mice that were intravitreally injected with AAV-CRMP2$^{T/A}$. Three weeks after AAV injection, animals were subjected to ONC+IS and killed 21 d thereafter. Asterisks indicate the lesion site. (Scale bar: 200 μm.) (*D*–*G*) Magnifications of optic nerve sections as indicated in *C* at 2 and 4 mm beyond the lesion site. (Scale bar: 200 μm.) (*H*) Quantification of regenerating axons at indicated distances beyond the crush site in optic nerves as described in *C*. In comparison with animals without AAV-CRMP2$^{T/A}$ injection (dashed lines; data from Fig. 2), CRMP2$^{T/A}$ significantly improved optic nerve regeneration in WT mice, but the effect was potentiated in $(\alpha/\beta)^{S/A}$ mice. Values represent means ± SEM of at least $n = 5$ animals per group. (*I*–*L*) Two sections of the chiasm attached to the optic nerve from the same CRMP2$^{T/A}$ -treated $(\alpha/\beta)^{S/A}$ animal as shown in *C*, *F*, and *G*, with several axons reaching the chiasm. (*J* and *L*) Magnifications of the chiasm as indicated in *I* and *K*, respectively. Arrows indicate axons in the chiasm. Significances of intergroup differences were evaluated by three-way (*A*) or two-way (*B* and *H*) ANOVA followed by Tukey post hoc test. Treatment effects: $^{**}P < 0.01$ and $^{***}P < 0.001$. n.s., nonsignificant.

LCM concentrations; Fig. 4*H*). Significantly, upon RGC-specific CRMP2$^{T/A}$ expression in GSK3$(\alpha/\beta)^{S/A}$ mice, neurite growth was no longer decreased, but surprisingly rather increased on permissive substrate (~2.2-fold) and myelin extract (~5.2-fold) in comparison with the respective WT, suggesting that sufficient levels of active nonphosphorylated CRMP2 unmasked an otherwise hidden growth-promoting effect of active GSK3. Consistently, CRMP2$^{T/A}$ expression had no effect on MAP1B phosphorylation, as levels of pMAP1B in neurite growth cones of GSK3$(\alpha/\beta)^{S/A}$ were still markedly increased compared with WT controls (Fig. 5*B*). We also tested whether CRMP2$^{T/A}$ expression might similarly affect optic nerve regeneration. To this end, WT and GSK3$(\alpha/\beta)^{S/A}$ mice received intravitreal injections of AAV-CRMP2$^{T/A}$ 3 wk before ONC+IS. Similar to GSK3$\beta^{-/-}$, CRMP2$^{T/A}$ expression in WT animals markedly increased IS-stimulated axon regeneration (Fig. 5 *C*–*H* and Fig. S9). Strikingly, CRMP2$^{T/A}$ expression also converted the negative effect of GSK3$(\alpha/\beta)^{S/A}$ into the strongest regeneration measured in this study, with some axons reaching the optic chiasm as soon as 3 wk after injury (Fig. 5 *I*–*L*). The survival of RGCs was not significantly affected by CRMP2$^{T/A}$ overexpression (Fig. S3 *A* and *B*). Thus, as in the PNS, enhanced GSK3 activity significantly promotes CNS axon regeneration if its inhibitory activity on CRMP2 is circumvented.

GSK3 Activity Promotes Neurite Growth of Naïve RGCs in Culture. As CRMP2$^{T/A}$ expression converted the impact of GSK3 activity from a negative to a growth-promoting effect in vivo, we wondered whether enhanced GSK3 activity might also affect neurite growth of naïve RGCs without prior ONC treatment in vivo. These naïve RGCs were expected to display high pCRMP2 levels in the WT as well, based on the immunostaining of retinal flat-mounts (Fig. S8*A*). In contrast to conditions 5 d after axotomy in which pCRMP2 was significantly lower in the WT, we noted that cultured RGCs from untreated (naïve) WT, GSK3$\alpha^{S/A}$, GSK3$\beta^{S/A}$, and GSK3$(\alpha/\beta)^{S/A}$ mice showed unaltered high pCRMP2 levels (Fig. S7 *D* and *E*). Total CRMP2 levels in RGCs remained unchanged among all genotypes upon ONC and in naïve conditions (Fig. S7 *F* and *G*). As pCRMP2 levels did not decrease in WT RGCs as early as 3 d after culturing, these naïve cultures provided conditions to test the effects of GSK3 activity mostly independently of its impact on changes of endogenous CRMP2 activity (Fig. 6 *A* and *B*). We therefore prepared naïve cultures from WT, GSK3$\alpha^{S/A}$, GSK3$\beta^{S/A}$, and GSK3$(\alpha/\beta)^{S/A}$ mice and incubated them with or without CNTF

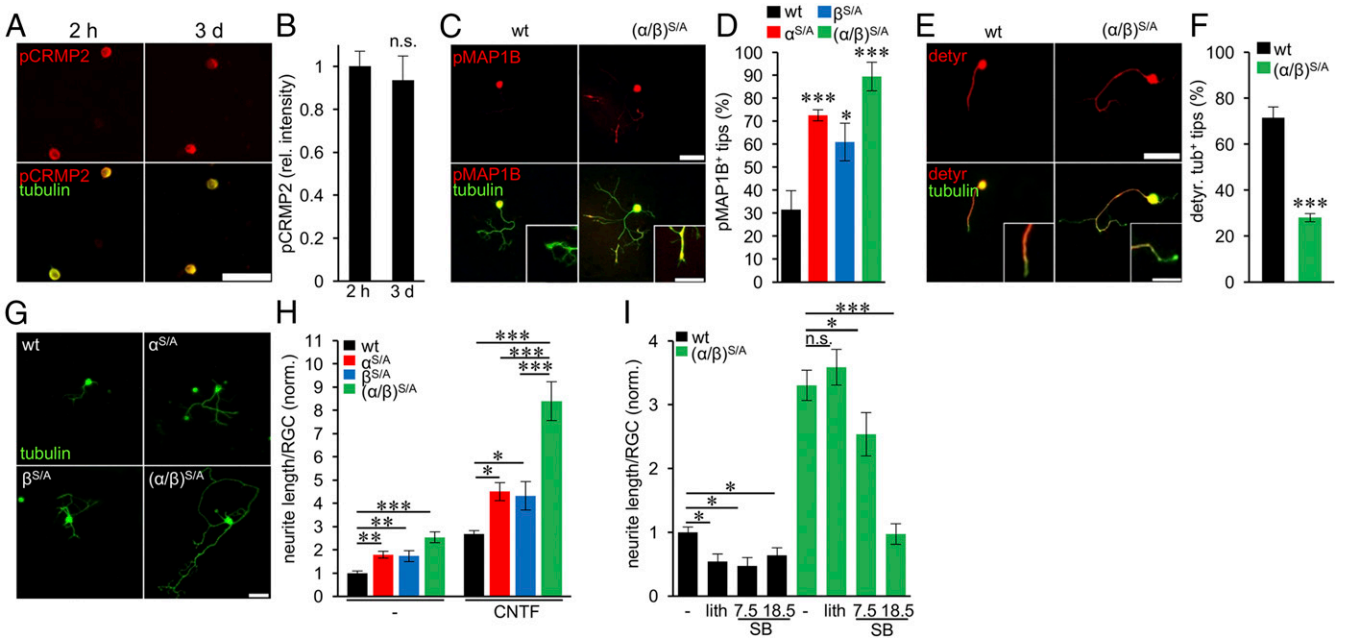

Fig. 6. GSK3 activity enhances RGC neurite growth and MAP1B phosphorylation in naïve retinal cultures. (*A*) Representative pictures of dissociated RGCs stained for T514-phosphorylated CRMP2 (pCRMP2; red) and βIII-tubulin (green) after 2 h or 3 d in culture. RGCs were isolated from untreated naïve WT retinae. pCRMP2 levels did not change over a time period of 3 d in culture. (Scale bar: 50 μm.) (*B*) Quantification of pCRMP2 staining intensities of RGCs as described in *A*. Values represent means ± SEM of $n = 3$ independent experiments per group. (*C*) Representative pictures of βIII-tubulin–positive RGCs (green) from WT and GSK3$(\alpha/\beta)^{S/A}$ [$(\alpha/\beta)^{S/A}$] mice costained for T1265-phosphorylated MAP1B (pMAP1B; red), which were cultured for 3 d in the presence of CNTF (200 ng/mL). (*Insets*) Higher magnification of respective neurite tips. (Scale bars: 50 μm; *Insets*, 15 μm.) (*D*) Quantification of the percentage of pMAP1B-positive neurite tips in RGC cultures as depicted in *C*. $\alpha^{S/A}$ and $\beta^{S/A}$ significantly increased the percentage of pMAP1B-positive tips with strongest effects in $(\alpha/\beta)^{S/A}$ RGCs. Data represent means ± SEM of $n = 3$ independent experiments. (*E*) Representative pictures of βIII-tubulin–positive RGCs (green) as described in *C* stained for detyrosinated α-tubulin (detyr.; red). (*Insets*) Neurite tips at greater magnification. (Scale bars: 50 μm; *Insets*, 15 μm.) (*F*) Quantification of RGC neurite tips with detyrosinated α-tubulin staining as depicted in *E*. $(\alpha/\beta)^{S/A}$ significantly reduced microtubule detyrosination. Data represent means ± SEM of $n = 3$ independent experiments. (*G*) Representative pictures of βIII-tubulin–positive RGCs (tubulin; green) from untreated, naïve WT, $\alpha^{S/A}$, $\beta^{S/A}$, and $(\alpha/\beta)^{S/A}$ mice cultured for 3 d in the presence of CNTF (200 ng/mL). (Scale bar: 50 μm.) (*H*) Quantification of neurite growth of RGCs as described in *G* cultured in the absence and presence of CNTF. Neurite growth was increased in $\alpha^{S/A}$ and $\beta^{S/A}$ RGCs to the same extent and further in $(\alpha/\beta)^{S/A}$ RGCs compared with WT RGCs. Data represent means ± SEM of $n = 3$ independent experiments normalized to WT control with an average length of 2.82 μm per RGC. (*I*) Quantification of neurite growth of WT and $(\alpha/\beta)^{S/A}$ RGCs cultured in the presence of CNTF and GSK3 inhibitors lithium (lith; 3 mM) or SB415286 (SB; 7.5 and 18.5 μM). Data represent means ± SEM of $n = 3$ independent experiments normalized to only CNTF-treated WT RGCs with a neurite length of 8.17 μm per RGC. Significances of intergroup differences were evaluated by using one-way (*D*) or two-way (*H* and *I*) ANOVA with Tukey post hoc test or Student's *t* test (*B* and *F*). Treatment effects: $*P < 0.05$, $**P < 0.01$, and $***P < 0.001$. n.s., nonsignificant.

for 3 d to enable neurite growth. Indeed, under these conditions, mean neurite growth was significantly longer for GSK3$\alpha^{S/A}$ and GSK3$\beta^{S/A}$ RGCs and strongest (~2.5 fold) for GSK3$(\alpha/\beta)^{S/A}$ RGCs compared with WT controls. Similar relative effects were observed upon additional treatment with CNTF, which was used to stimulate the cell-intrinsic growth state, like IS in the previously used paradigms (Fig. 6 *G* and *H*). Enhanced neurite growth correlated with the degree of MAP1B phosphorylation in neurite growth cones, indicating increasing GSK3 activity in GSK3$(\alpha/\beta)^{S/A}$ compared with GSK3$\alpha^{S/A}$ and GSK3$\beta^{S/A}$ and WT RGCs (Fig. 6 *C* and *D*). Moreover, the growth-promoting effect of GSK3$(\alpha/\beta)^{S/A}$ was markedly compromised by SB415286, which directly inhibits GSK3 activity via blocking its substrate-binding site (37), but not by lithium, which increases AKT-mediated inhibitory phosphorylation of GSK3 (Fig. 6*I*). Thus, the kinase activity of GSK3 is essential for the neurite growth-promoting effect of GSK3$(\alpha/\beta)^{S/A}$. As pMAP1B reportedly increases microtubule dynamics by inhibiting detyrosination (27, 32, 38, 39), GSK3$(\alpha/\beta)^{S/A}$ consistently reduced the percentage of axonal tips with detyrosinated tubulin compared with WT controls (Fig. 6 *E* and *F*). These data demonstrate that, as previously shown for peripheral sensory neurons, elevated GSK3 activity can promote RGC neurite growth via reduction of microtubule detyrosination and subsequent increase in microtubule dynamics (32). However, this effect is normally masked in the CNS by a dominant effect of endogenous CRMP2 inhibition.

Discussion

The present study investigated the role of both GSK3 isoforms and two of their downstream targets in CNS axon regeneration, taking advantage of various genetic mouse models and the classical optic nerve injury paradigm. In contrast to improvement of sciatic nerve regeneration (22, 32), the sustained GSK3 activity in GSK3$^{S/A}$ mice compromised IS-stimulated optic nerve regeneration without affecting the expression of regeneration-associated genes or neuronal survival. This diverging outcome was evidently based on much stronger GSK3-mediated CRMP2 inactivation in axons of the central optic nerve than the peripheral sciatic nerve, thus impeding axon regeneration. The negative effect of GSK3 on CRMP2 activity superimposed its beneficial effect via pMAP1B-associated reduction of microtubule detyrosination. Accordingly, optic nerve regeneration was dramatically improved in GSK3$^{S/A}$ mice upon neutralization of CRMP2 inhibition. Therefore, these insights into the antagonistic effects of GSK3 activity reconcile the so far inconsistent reports on the role of GSK3 in PNS and CNS axon regeneration. Moreover, combination of the positive effects of activation and inhibition of GSK3 open promising options for novel therapeutic interventions for CNS repair.

GSK3 has long been implicated in axon regeneration, even though its exact role has been controversial (23). Surprisingly, only few previous studies analyzed the regulation of GSK3 itself upon nerve injury. Inhibitory phosphorylation of GSK3α^{S21} and GSK3β^{S9} is markedly increased in axotomized sensory neurons and their regenerating axons (22, 40). In contrast to a previous report (18), here we detected, similar to the PNS (22), significant induction of GSK3 phosphorylation in somata and axons of RGCs at 5 d after ONC using specificity-verified antibodies. Consistent with axotomy-induced inhibition, GSK3-mediated CRMP2 phosphorylation decreased after injury. Similarly, pCRMP2 levels were reduced in GSK3β$^{-/-}$ mice, whereas pCRMP2 and pMAP1B were expectedly increased in GSK3$^{S/A}$ mice compared with WT controls, confirming the dependency of their phosphorylation on overall GSK3 activity. The observed slight decrease of pCRMP2 in optic nerves of GSK3(α/β)$^{S/A}$ mice after ONC suggests that additional mechanisms might also be involved in the injury-induced regulation of this substrate (41).

We recently demonstrated that the axon growth-promoting effect of GSK3$^{S/A}$ in sensory neurons was attributed to reduced tubulin detyrosination upon GSK3-mediated MAP1B activation, whereas almost no pCRMP2 was detectable in sciatic nerves of WT or even GSK3$^{S/A}$ animals (32). In contrast to the PNS, the present study found relatively high levels of pCRMP2 in optic nerve axons of uninjured WT mice, which were further increased by active GSK3$^{S/A}$ and compromised axonal regeneration in vivo. It is therefore likely that priming kinases, such as CDK5, that are required for subsequent CRMP2 phosphorylation by GSK3 (41–43) have different activities in the CNS and PNS. Consistently, CDK5 is reportedly active in the CNS and even in DRG harboring the somata, but inactive in the sciatic nerve with the axons (44). Despite the present lack of knowledge about whether CDK5-dependent CRMP2 priming is involved in this process, our findings suggest that GSK3-mediated inactivation of axonal CRMP2 is rather irrelevant for peripheral nerve regeneration, but plays a dominant role in the CNS. In agreement with this idea, reduced CRMP2 phosphorylation correlated with improved axon regeneration in GSK3β$^{-/-}$ mice, and increased CRMP2 phosphorylation reduced regeneration in GSK3$^{S/A}$ compared with WT mice. Moreover, expression of nonphosphorylatable CRMP2$^{T/A}$ mostly mimicked disinhibition and growth promotion of GSK3β$^{-/-}$, while a CRMP2 inhibitor abrogated these effects, thereby verifying its functional relevance.

Overcoming myelin growth inhibition is an important aspect of successful CNS regeneration, and CRMP2 has previously been reported to counteract the negative effect of inhibitory molecules, such as myelin-associated factors or chondroitin sulfate proteoglycans (20, 25). Generally, disinhibitory treatments on their own are not very effective, but can facilitate optic nerve regeneration in combination with procedures elevating the regenerative state of RGCs, such as IS (10, 14, 45). Accordingly, GSK3β$^{-/-}$ as well as CRMP2$^{T/A}$ expression effectively promoted optic nerve regeneration particularly in combination with IS. The essential role of CRMP2 for neurite growth and disinhibition was confirmed in cell-culture experiments with primary RGCs. Application of the CRMP2 inhibitor LCM (35, 36) reduced neurite growth of WT RGCs. However, RGCs had to be prestimulated in vivo to increase the activity level of CRMP2 (reduction of CRMP2 phosphorylation). As RGCs isolated from GSK3$^{S/A}$ mice showed high levels of inactive pCRMP2 despite prestimulation, LCM was ineffective in these cells. On the contrary, GSK3β$^{-/-}$ RGCs with highly active CRMP2 showed increased neurite growth. This effect was therefore blocked by LCM, particularly when RGCs were cultured on inhibitory CNS myelin. Accordingly, CRMP2$^{T/A}$ expression also mainly promoted RGC growth on inhibitory myelin, which is consistent with the role of CRMP2 in disinhibition (20, 25). Thus, the potentiating effect of GSK3β$^{-/-}$ or CRMP2$^{T/A}$ expression on IS-induced optic nerve regeneration might be predominantly attributable to disinhibitory effects toward myelin or potentially other inhibitors.

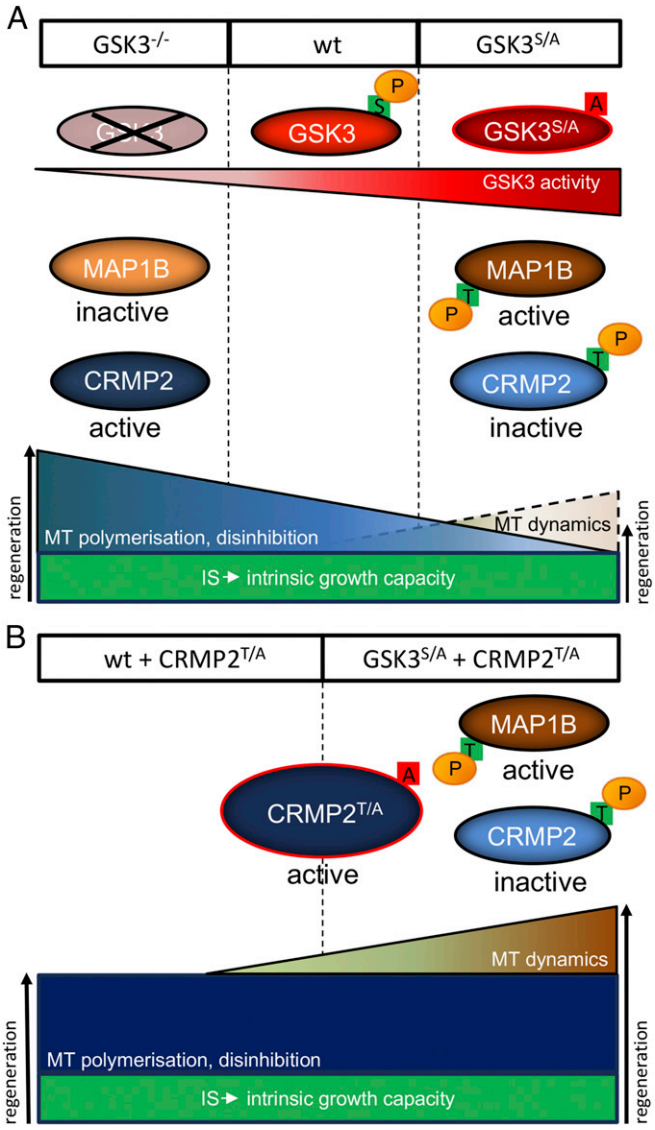

Fig. 7. Complementary modulation of antagonistic effects of GSK3 synergistically promotes CNS axon regeneration. (*A*) IS activates the intrinsic growth program of RGCs and moderately promotes optic nerve regeneration independent of GSK3 activity (green box). Phosphorylation of GSK3 regulates its kinase activity (red triangle), which in turn controls the activity of the microtubule-binding proteins CRMP2 and MAP1B. GSK3-mediated phosphorylation inactivates CRMP2, thereby abolishing its microtubule (MT) polymerization promoting and disinhibitory effects (blue triangle). On the contrary, GSK3 phosphorylation activates MAP1B, increasing microtubules dynamics in axonal growth cones by reducing tubulin detyrosination (brown triangle). Increased MT polymerization, disinhibition, and MT dynamics all improve axon regeneration, but are inversely regulated by GSK3 activity. As shown by the present study, GSK3 depletion (GSK3$^{-/-}$) increases CRMP2 activity, resulting in enhanced axon regeneration. Moreover, the role of active CRMP2 appears to be dominating in this context in the CNS. The positive effect of constitutively active GSK3 (GSK3$^{S/A}$) on pMAP1B/microtubule detyrosination is masked and can only partially compensate the negative impact of GSK3-mediated CRMP2 phosphorylation. (*B*) Overexpression of nonphosphorylatable CRMP2 (CRMP2$^{T/A}$) enhances MT polymerization and disinhibition independent of GSK3 activity. Thus, inactivation of endogenous CRMP2 upon constitutively active GSK3 (GSK3$^{S/A}$) becomes irrelevant, and the increase of MT dynamics under these conditions further promotes axon regeneration.

Interestingly, only GSK3β$^{-/-}$, but not GSK3α$^{-/-}$, decreased CRMP2 phosphorylation, which was particularly evident upon ONC. This result is consistent with a previous study describing reduced CRMP2 phosphorylation in CNS neurons upon GSK3β$^{-/-}$, but not GSK3α$^{-/-}$ (46). Although both isoforms are reportedly able to phosphorylate primed CRMP2, GSK3α is considered less active in vivo (46, 47) and can apparently not substitute for GSK3β in respective KO animals. In contrast, constitutively active GSK3α$^{S/A}$ was seemingly as active as GSK3β$^{S/A}$, because CRMP2 and MAP1B were comparably phosphorylated in the two single knock-in mice. Overall, our data demonstrate an inverse correlation between GSK3 activity, CRMP2 phosphorylation, and axon regeneration in vivo.

Strikingly, increased GSK3 activity also promoted axon regeneration of RGCs, most likely similar to DRG neurons via pMAP1B-associated inhibition of tubulin detyrosination, when the influence of CRMP2 activity was experimentally neutralized (i.e., balanced pCRMP2 levels in naïve cell cultures or expression of constitutively active CRMP2$^{T/A}$). This effect on microtubule detyrosination is also likely the underlying cause for the less pronounced reduction of optic nerve regeneration in GSK3$^{S/A}$ double compared with single knock-in mice (Fig. 2 *D* and *I*), as CRMP2 inhibition was seemingly already maximal upon single knock-in. Thus, the beneficial effect of MAP1B activation in GSK3$^{S/A}$ mice on CNS axon regeneration is normally superimposed by the negative effect of CRMP2 phosphorylation, and unmasked by CRMP2$^{T/A}$ overexpression (Fig. 7). In fact, combination of active CRMP2 and inhibition of tubulin detyrosination markedly potentiated IS-mediated optic nerve regeneration in GSK3$^{S/A}$ mice, enabling stronger regeneration than GSK3β$^{-/-}$ or CRMP2$^{T/A}$ expression alone (Fig. 7). In comparison with our previously published data on the regenerative effects of PTEN KO and PTEN KO+IS, respectively, in the same mouse background (48), regeneration achieved here by GSK3β$^{-/-}$ or CRMP2$^{T/A}$+IS was distinctly stronger. Whether additional neuroprotective treatments or longer than 3 wk of regeneration would enable growth beyond the optic chiasm and ultimately lead to reinnervation of RGC targets needs to be addressed in the future. Moreover, PTEN depletion activates AKT, which acts upstream of GSK3 and CRMP2, leaving the possibility that both proteins participate in axon growth stimulation by PTEN KO (18, 49). Studies addressing these potential interactions are currently under way.

Despite these remaining questions, the concept of complementary modulation of normally antagonistically targeted GSK3 substrates might open new therapeutic strategies for CNS repair. In this respect, it might be more feasible to combine parthenolide, which mimics the effects of GSK3 activation by direct inhibition of tubulin detyrosination (32), with pharmacological GSK3 inhibition, for example, by lithium, to reduce CRMP2 inactivation and efficient activation of the intrinsic growth potential, for example, with IS or hyper–IL-6 (48). Future studies will address the feasibility and outcome of such combinatorial pharmacological strategies to promote optic nerve and more general CNS regeneration.

Materials and Methods

Animals and surgical procedures were approved by the local animal care committee (Landesamt für Natur, Umwelt, und Verbraucherschutz Recklinghausen) and conducted in compliance with federal and state guidelines for animal experiments in Germany. Housing conditions, mouse strains, and surgical procedures are described in *SI Materials and Methods*.

Western Blot Assays. For protein lysate preparation, mice were killed, and tissues were isolated and dissected. Retinae, optic nerves, or sciatic nerves were homogenized in lysis buffer, and cleared by centrifugation. Proteins were separated by SDS/PAGE according to standard protocols and transferred to nitrocellulose membranes (0.2 μm; Bio-Rad). Details on Western blot analysis, antibodies, and signal quantification are described in *SI Materials and Methods*.

Immunohistochemistry. Animals were intracardially perfused with cold saline solution followed by PBS solution containing 4% paraformaldehyde (PFA). The tissue was then embedded in KP-cryo compound (Klinipath), and sections were cut on a cryostat. Details on the protocol and antibodies used are described in *SI Materials and Methods*.

Quantification of Axons in the Optic Nerve. Regeneration of axons was quantified over the entire length of the optic nerve for all animals as previously described (11, 12). Details on quantification are described in *SI Materials and Methods*.

Quantification of RGCs in Retinal Whole-Mounts. For quantification of surviving RGCs, retinal whole-mounts were immunohistochemically stained, and the average density of RGCs was determined. Details are described in *SI Materials and Methods*.

Preparation of AAV2. Details on recombinant AAV2 (afterward referred to as AAV) production are described in *SI Materials and Methods*.

RNA Isolation and Quantitative Real-Time PCR. Total RNA was isolated from mouse retinae and reverse-transcribed. Expression of Gap43, Galanin, Sprr1a, and GAPDH was then quantified by real-time PCR. Details and primers are described in *SI Materials and Methods*.

Dissociated Retinal Cell Cultures. For experiments requiring in vivo pretreatment, mice were subjected to ONC or ONC+IS. Five days thereafter, retinal cultures were prepared as described previously (50). In experiments without prior in vivo treatment, retinal cells of respective genotypes were isolated as described earlier. After trituration, the cell suspension of one retina was immediately washed with 50 mL DMEM to remove cell fragments or factors released from the cells and centrifuged for 7 min at 500 × *g*. Details on culture preparation, factors and antibodies, as well as quantification of neurite growth are described in *SI Materials and Methods*.

Quantification of pMAP1B- and Detyrosinated Tubulin-Positive Axon Tips in Retinal Cultures. Details on the methods and antibodies used are described in *SI Materials and Methods*.

Quantification of CRMP2 and pCRMP2 Immunostaining in Cultured RGCs. Methodological details and antibodies used are described in *SI Materials and Methods*.

Statistical Analysis. Significances of intergroup differences were evaluated by using Student's *t* test or ANOVA followed by Holm–Šídák or Tukey post hoc test by using GraphPad Prism software.

ACKNOWLEDGMENTS. We thank Prof. Dr. Dario Alessi for providing the GSK3β knock-in mice, Prof. Dr. James R. Woodget for providing the GSK3β-floxed mice, and Marcel Kohlhaas for technical support. This work was supported by the German Research Foundation.

1. Fischer D, Leibinger M (2012) Promoting optic nerve regeneration. *Prog Retin Eye Res* 31:688–701.
2. Silver J, Miller JH (2004) Regeneration beyond the glial scar. *Nat Rev Neurosci* 5:146–156.
3. Lu Y, Belin S, He Z (2014) Signaling regulations of neuronal regenerative ability. *Curr Opin Neurobiol* 27:135–142.
4. Leibinger M, et al. (2009) Neuroprotective and axon growth-promoting effects following inflammatory stimulation on mature retinal ganglion cells in mice depend on ciliary neurotrophic factor and leukemia inhibitory factor. *J Neurosci* 29:14334–14341.
5. Müller A, Hauk TG, Fischer D (2007) Astrocyte-derived CNTF switches mature RGCs to a regenerative state following inflammatory stimulation. *Brain* 130:3308–3320.
6. Fischer D, Pavlidis M, Thanos S (2000) Cataractogenic lens injury prevents traumatic ganglion cell death and promotes axonal regeneration both in vivo and in culture. *Invest Ophthalmol Vis Sci* 41:3943–3954.
7. Yin Y, et al. (2003) Macrophage-derived factors stimulate optic nerve regeneration. *J Neurosci* 23:2284–2293.
8. Leibinger M, et al. (2013) Interleukin-6 contributes to CNS axon regeneration upon inflammatory stimulation. *Cell Death Dis* 4:e609.
9. Hauk TG, et al. (2010) Stimulation of axon regeneration in the mature optic nerve by intravitreal application of the toll-like receptor 2 agonist Pam3Cys. *Invest Ophthalmol Vis Sci* 51:459–464.
10. Fischer D, Petkova V, Thanos S, Benowitz LI (2004) Switching mature retinal ganglion cells to a robust growth state in vivo: Gene expression and synergy with RhoA inactivation. *J Neurosci* 24:8726–8740.
11. Leibinger M, Andreadaki A, Fischer D (2012) Role of mTOR in neuroprotection and axon regeneration after inflammatory stimulation. *Neurobiol Dis* 46: 314–324.

12. Leibinger M, Andreadaki A, Diekmann H, Fischer D (2013) Neuronal STAT3 activation is essential for CNTF- and inflammatory stimulation-induced CNS axon regeneration. *Cell Death Dis* 4:e805.
13. Diekmann H, Fischer D (2013) Glaucoma and optic nerve repair. *Cell Tissue Res* 353: 327–337.
14. Fischer D, He Z, Benowitz LI (2004) Counteracting the Nogo receptor enhances optic nerve regeneration if retinal ganglion cells are in an active growth state. *J Neurosci* 24:1646–1651.
15. Sengottuvel V, Leibinger M, Pfreimer M, Andreadaki A, Fischer D (2011) Taxol facilitates axon regeneration in the mature CNS. *J Neurosci* 31:2688–2699.
16. Heskamp A, et al. (2013) CXCL12/SDF-1 facilitates optic nerve regeneration. *Neurobiol Dis* 55:76–86.
17. Dill J, Wang H, Zhou F, Li S (2008) Inactivation of glycogen synthase kinase 3 promotes axonal growth and recovery in the CNS. *J Neurosci* 28:8914–8928.
18. Guo X, Snider WD, Chen B (2016) GSK3β regulates AKT-induced central nervous system axon regeneration via an eIF2Bε-dependent, mTORC1-independent pathway. *eLife* 5:e11903.
19. Alabed YZ, Pool M, Ong Tone S, Sutherland C, Fournier AE (2010) GSK3 beta regulates myelin-dependent axon outgrowth inhibition through CRMP4. *J Neurosci* 30: 5635–5643.
20. Liz MA, et al. (2014) Neuronal deletion of GSK3β increases microtubule speed in the growth cone and enhances axon regeneration via CRMP-2 and independently of MAP1B and CLASP2. *BMC Biol* 12:47.
21. Miao L, et al. (2016) mTORC1 is necessary but mTORC2 and GSK3β are inhibitory for AKT3-induced axon regeneration in the central nervous system. *eLife* 5:e14908.
22. Gobrecht P, Leibinger M, Andreadaki A, Fischer D (2014) Sustained GSK3 activity markedly facilitates nerve regeneration. *Nat Commun* 5:4561.
23. Diekmann H, Fischer D (2015) Role of GSK3 in peripheral nerve regeneration. *Neural Regen Res* 10:1602–1603.
24. Cole AR, et al. (2008) Relative resistance of Cdk5-phosphorylated CRMP2 to dephosphorylation. *J Biol Chem* 283:18227–18237.
25. Nagai J, Owada K, Kitamura Y, Goshima Y, Ohshima T (2016) Inhibition of CRMP2 phosphorylation repairs CNS by regulating neurotrophic and inhibitory responses. *Exp Neurol* 277:283–295.
26. Seira O, Del Río JA (2014) Glycogen synthase kinase 3 beta (GSK3β) at the tip of neuronal development and regeneration. *Mol Neurobiol* 49:931–944.
27. Trivedi N, Marsh P, Goold RG, Wood-Kaczmar A, Gordon-Weeks PR (2005) Glycogen synthase kinase-3beta phosphorylation of MAP1B at Ser1260 and Thr1265 is spatially restricted to growing axons. *J Cell Sci* 118:993–1005.
28. Scales TM, Lin S, Kraus M, Goold RG, Gordon-Weeks PR (2009) Nonprimed and DYRK1A-primed GSK3 beta-phosphorylation sites on MAP1B regulate microtubule dynamics in growing axons. *J Cell Sci* 122:2424–2435.
29. Kim WY, et al. (2006) Essential roles for GSK-3s and GSK-3-primed substrates in neurotrophin-induced and hippocampal axon growth. *Neuron* 52:981–996.
30. Hur EM, Zhou FQ (2010) GSK3 signalling in neural development. *Nat Rev Neurosci* 11: 539–551.
31. McManus EJ, et al. (2005) Role that phosphorylation of GSK3 plays in insulin and Wnt signalling defined by knockin analysis. *EMBO J* 24:1571–1583.
32. Gobrecht P, et al. (2016) Promotion of functional nerve regeneration by inhibition of microtubule detyrosination. *J Neurosci* 36:3890–3902.
33. Lingor P, et al. (2008) ROCK inhibition and CNTF interact on intrinsic signalling pathways and differentially regulate survival and regeneration in retinal ganglion cells. *Brain* 131:250–263.
34. Dergham P, et al. (2002) Rho signaling pathway targeted to promote spinal cord repair. *J Neurosci* 22:6570–6577.
35. Park KD, et al. (2009) Lacosamide isothiocyanate-based agents: Novel agents to target and identify lacosamide receptors. *J Med Chem* 52:6897–6911.
36. Wilson SM, et al. (2012) Prevention of posttraumatic axon sprouting by blocking collapsin response mediator protein 2-mediated neurite outgrowth and tubulin polymerization. *Neuroscience* 210:451–466.
37. Coghlan MP, et al. (2000) Selective small molecule inhibitors of glycogen synthase kinase-3 modulate glycogen metabolism and gene transcription. *Chem Biol* 7: 793–803.
38. Goold RG, Owen R, Gordon-Weeks PR (1999) Glycogen synthase kinase 3beta phosphorylation of microtubule-associated protein 1B regulates the stability of microtubules in growth cones. *J Cell Sci* 112:3373–3384.
39. Barnat M, et al. (2016) The GSK3-MAP1B pathway controls neurite branching and microtubule dynamics. *Mol Cell Neurosci* 72:9–21.
40. Saijilafu, et al. (2013) PI3K-GSK3 signalling regulates mammalian axon regeneration by inducing the expression of Smad1. *Nat Commun* 4:2690.
41. Yoshimura T, et al. (2005) GSK-3beta regulates phosphorylation of CRMP-2 and neuronal polarity. *Cell* 120:137–149.
42. Soutar MP, Thornhill P, Cole AR, Sutherland C (2009) Increased CRMP2 phosphorylation is observed in Alzheimer's disease; does this tell us anything about disease development? *Curr Alzheimer Res* 6:269–278.
43. Cole AR, et al. (2006) Distinct priming kinases contribute to differential regulation of collapsin response mediator proteins by glycogen synthase kinase-3 in vivo. *J Biol Chem* 281:16591–16598.
44. Terada M, et al. (1998) Expression and activity of cyclin-dependent kinase 5/p35 in adult rat peripheral nervous system. *J Neurochem* 71:2600–2606.
45. Sengottuvel V, Fischer D (2011) Facilitating axon regeneration in the injured CNS by microtubules stabilization. *Commun Integr Biol* 4:391–393.
46. Soutar MP, et al. (2010) Evidence that glycogen synthase kinase-3 isoforms have distinct substrate preference in the brain. *J Neurochem* 115:974–983.
47. Cole A, Frame S, Cohen P (2004) Further evidence that the tyrosine phosphorylation of glycogen synthase kinase-3 (GSK3) in mammalian cells is an autophosphorylation event. *Biochem J* 377:249–255.
48. Leibinger M, Andreadaki A, Gobrecht P, Levin E, Fischer D (2016) Boosting CNS axon regeneration by circumventing limitations of natural cytokine signaling. *Mol Ther* 24: 1712–1725.
49. Park KK, et al. (2008) Promoting axon regeneration in the adult CNS by modulation of the PTEN/mTOR pathway. *Science* 322:963–966.
50. Grozdanov V, Muller A, Sengottuvel V, Leibinger M, Fischer D (2010) A method for preparing primary retinal cell cultures for evaluating the neuroprotective and neuritogenic effect of factors on axotomized mature CNS neurons. Curr Protoc Neurosci Chapter 3:Unit 3.22.